A CRISPR-based assay for the detection of opportunistic infections post-transplantation and for the monitoring of transplant rejection

A CRISPR-based assay for the detection of opportunistic infections post-transplantation and for the monitoring of transplant rejection

Michael M. Kaminski[1,2,3], Miguel A. Alcantar[1], Isadora Lape[4], Robert Greensmith[2,3], Allison C. Huske[1], Jacqueline A. Valeri[1,9], Francisco M. Marty[5], Verena Klämbt[6], Jamil Azzi[4], Enver Akalin[7], Leonardo V. Riella[4*], and James J. Collins[1,8,9*]

Abstract

In organ transplantation, infection and rejection are major causes of graft loss linked by the net state of immunosuppression. To diagnose and treat these conditions earlier, and to improve long-term patient outcomes, refined strategies for the monitoring of patients after graft transplantation are needed. Here, we show that a fast and inexpensive assay based on CRISPR-Cas13 accurately detects BK polyomavirus DNA and cytomegalovirus DNA from patient-derived blood and urine samples, as well as CXCL9 mRNA (a marker of graft rejection) at elevated levels in urine samples from patients experiencing acute renal-transplant rejection. The assay, which we adapted for lateral-flow readout, enables via simple visualization the post-transplantation monitoring of common opportunistic viral infections and of graft rejection, and should facilitate point-of-care post-transplantation monitoring.

[1]Institute for Medical Engineering and Science and Department of Biological Engineering, Massachusetts Institute of Technology, Cambridge, MA 02139, USA. [2]Berlin Institute for Medical Systems Biology, Max Delbrück Center for Molecular Medicine in the Helmholtz Association, 10115 Berlin, Germany. [3]Department of Nephrology and Medical Intensive Care, Charité - Universitätsmedizin Berlin, 10117 Berlin, Germany. [4]Schuster Transplantation Research Center, Brigham & Women's Hospital, Harvard Medical School, Boston, MA 02115, USA. [5]Division of Infectious Diseases, Brigham and Women's Hospital, Boston, MA 02115, USA. [6]Department of Medicine, Boston Children's Hospital, Harvard Medical School, Boston, MA 02115, USA. [7]Montefiore Einstein Center for Transplantation, Montefiore Medical Center, Albert Einstein College of Medicine, Bronx, New York 10467, USA. [8]Infectious Disease and Microbiome Program, Broad Institute of MIT and Harvard, Cambridge, MA 02142, USA. [9]Wyss Institute for Biologically Inspired Engineering, Harvard University, Boston, MA 02115, USA. *corresponding authors, e-mail: jimjc@mit.edu, lriella@bwh.harvard.edu

Main

The clustered regularly interspaced short palindromic repeats (CRISPR) and CRISPR-associated (Cas) immune system has recently been adapted for the detection of nucleic acids[1–8]. These protocols enable rapid, cost-effective DNA and RNA detection in a variety of sample

types with excellent sensitivity and specificity, making them ideal tools for point-of-care (POC) testing. However, most studies to date have used synthetic standards, include few clinical specimens, and lack direct comparison to clinical gold standard diagnostics.
Here, we applied and optimized the CRISPR-Cas13 SHERLOCK (specific high-sensitivity enzymatic reporter unlocking) technology for diagnosis of biomarkers highly relevant for renal transplant patients.

Since the first successful kidney transplantation in 1954, significant improvements in short-term outcomes have been achieved in organ transplantation. However, there has been less progress in long-term outcomes with more than half of the transplanted organs being lost after 10 years[9,10]. Opportunistic infections and transplant organ rejection are leading causes of graft loss, requiring careful adjustment of immunosuppression and life-long monitoring of post-transplant patients[11].

Current diagnostics, however, involve the use of expensive laboratory equipment and intricate multi-step protocols leading to limited availability, high costs and slow turn-around time[12,13]. Diagnosis of infections by PCR can take several days in clinical settings, and rejection diagnostics require invasive biopsies and histopathological analysis. These factors result in delays in pertinent diagnoses and increase the risk of irreversible allograft injury, especially in resource-limited settings. POC or at-home testing could significantly reduce associated costs and allow for more frequent monitoring, which would lead to earlier diagnosis and treatment of graft dysfunction and common infections.

In this study, we developed CRISPR-based diagnostic tools for cytomegalovirus (CMV) and BK polyomavirus (BKV) infection, two common opportunistic viruses highly relevant for renal transplant patients[14] and other immunocompromised patients[15,16]. Testing of more than 100 clinical specimens from BKV and CMV infected patients over a wide range of virus loads revealed high diagnostic accuracy. We further extended the capability of SHERLOCK to the detection of human *CXCL9* mRNA, a biomarker indicative of rejection in renal transplant patients[17–19]. We anticipate that CRISPR-Cas13-based technologies will be broadly applicable for personalized medicine diagnostics, where repeated testing of biomarkers indicative of disease activity is key to early and effective secondary prevention.

Results

Optimization of the CRISPR-Cas13 SHERLOCK technology for the detection of BKV and CMV virus from patient samples

To test for active BKV and CMV infection, we isolated DNA from blood and urine of both infected patients and uninfected control patients (Fig. 1a). Subsequently, we applied a modified version of the SHERLOCK protocol for BKV and CMV detection. In brief, conserved regions of BKV and CMV were amplified using isothermal recombinase polymerase amplification (RPA). Incorporation of the T7 promoter sequence into forward primers allowed for subsequent in-vitro RNA transcription using T7 polymerase. A CRISPR guide RNA (crRNA) complimentary to 28 nucleotides of the RPA product was used to direct Cas13 from *Leptotrichia wadei* (LwaCas13a) to the target sequence. Detection of the target resulted in Cas13 activation and subsequent collateral cleavage of an oligonucleotide carrying a quenched fluorophore, whose fluorescence can be measured upon cleavage and correlates with the initial target concentration present in the patient sample[1].

To identify conserved regions in the BKV genome, we aligned all strains accessible from the National Center for Biotechnology Information (NCBI) and focused on target regions with sequence homology of more than 95% among all strains (Fig. 1b). Next, we tested 12 different primer pairs and 3 crRNAs for detection of the BKV genes STA, VP2 and VP3 (Supplementary Fig.1a). We identified a crRNA-primer pair specific for the small T antigen (STA), which allowed detection of the *American Type Culture Collection* (ATCC) quantitative synthetic BKV standard (Dunlop strain) down to the low atto-molar range (0.3 aM), representing single-molecule detection in the assay volumes used (Figs. 1c,d). Importantly, systematic assessment of various forward and reverse primer concentrations (Supplementary Fig.1b) revealed a 120/480nM forward/reverse RPA primer concentration to be most sensitive. Using a similar strategy, we identified a conserved region in the CMV UL54 gene (Fig. 1e) as a potential SHERLOCK target which enabled detection of the ATCC diagnostic CMV standard (strain AD-169) down to the low atto-molar range (0.6 aM) (Figs. 1f,g).

Next, we tested if the diagnostic performance of the SHERLOCK assay would be sufficient to detect BKV and CMV virus in urine and plasma samples from patients. Testing of 31 urine and 36 plasma samples showed that the optimized SHERLOCK protocol correctly identified all BKV specimens with 100% sensitivity and specificity (Figs 2a,b, Supplementary Fig.2a). Importantly, this performance could be achieved using the rapid and simple HUDSON (heating unextracted

diagnostic samples to obliterate nucleases) protocol[2], which involves heating of the sample for 10 min at 95°C in the presence of TCEP and EDTA, circumventing the need for time-consuming, column-based sample preparations (Supplementary Figs. 2b,c).

Similarly, the CRISPR assay allowed for detection of CMV positive plasma samples with high sensitivity and specificity (Figs. 2c,d, Supplementary Figs.2b,c). In contrast to our BKV results, this performance could only be achieved using a commercial column-based viral DNA isolation kit, whereas the HUDSON protocol resulted in lower sensitivity for low copy number samples (< 1500 IU/mL). Likely, this difference in sensitivity is due to a sample concentration step included in the column-based kit.

CRISPR-based detection of *CXCL9* mRNA as a biomarker of kidney graft rejection

Next, we tested whether SHERLOCK could be applied to detect mRNA biomarkers indicative of kidney graft rejection. We selected *CXCL9* mRNA as a marker of rejection based on its validation in multicenter studies[17,18,20].

For detection of *CXCL9* mRNA, we isolated RNA from pelleted urine cells (Fig. 3a). For amplification, we included a reverse transcriptase into the RPA reaction (rtRPA). Using a synthetic RNA standard, Cas13 alone was sufficient to detect *CXCL9* in the low pico-molar range similar to the previously reported sensitivity (Fig. 3b). Addition of a rtRPA reaction followed by T7 transcription and Cas13 activation enabled *CXCL9* detection in the atto-molar range (Fig. 3b).

We next assessed whether this sensitivity was sufficient to discriminate patients undergoing kidney rejection (n=14) from a control group (n=17) (Supplementary Table 1). Importantly, rejection status was determined by gold standard kidney biopsy (Supplementary Table 2). We observed higher *CXCL9* mRNA levels in samples from patients with biopsy-proven rejection compared to transplant patients with no rejection or stable graft function, which allowed for the detection of kidney rejection with a sensitivity of 93% (Figs. 3c,d). The area under the receiver-operating-characteristic (ROC) curve (AUC) was 0.91 (Fig. 3e).

We confirmed *CXCL9* mRNA upregulation in rejection samples with the qPCR gold-standard assay[18] observing higher diagnostic accuracy relative to the CRISPR-based assay (Supplementary Figs. 3a,b,c). Detection of CXCL9 protein with an enzyme-linked

immunosorbent assay (ELISA) showed lower sensitivity but higher specificity (Supplementary Figs. 3d,e,f) as compared to CRISPR-based mRNA detection.

Rapid DNA isolation, CRISPR diagnostics and smartphone-based lateral-flow evaluation allow POC-ready detection of BKV and CMV infection

Point-of-care testing (POCT) holds great promise for transplantation medicine since fast and low-cost diagnostics could enable earlier treatment decisions and broader accessibility, thereby lowering the risk of irreversible transplant injury. To optimize BKV and CMV detection for POCT, we combined the rapid HUDSON DNA isolation protocol with SHERLOCK-based target detection and commercially available lateral-flow dipsticks (Fig. 4a). This method enabled an easy-to-read visual output that indicated a positive or negative test result. Since we observed that background noise can result in a faint test band on the lateral flow strip, we developed a smartphone-based software application that allowed quantification of band intensities (Supplementary video 1). Here, the software calculates the ratio of test to control band intensities using images taken with a smartphone camera, enabling simple and rapid discrimination between negative and positive test results. The total turn-around time from isolation to sample detection was below 2 hours.

We next tested the lateral-flow read-out for the detection of the CMV and BKV synthetic standard (Figs. 4b,c). Similar to our fluorescence-based read-out, we could detect both targets down to the atto-molar range. We set the relative band intensity cut-off discriminating a positive from a negative test result to 0.5, which corresponded to an interpolated concentration of 2.3 aM for the CMV standard and 0.5 aM for the BKV standard.

Using this protocol, we were able to detect CMV (Fig. 4d) and BKV (Fig. 4e) at different concentrations in patient samples. Although faint test bands were observable at very low concentrations, they were below the band intensity cut-off and thus classified as negative. Further, lateral flow-based CRISPR diagnostics successfully identified BKV infection in a 58-year-old male kidney transplant patient who was admitted for graft dysfunction. A kidney biopsy demonstrated BKV nephropathy and qPCR confirmed high viral BKV titers in the blood. After treatment, we could not detect BKV using CRISPR-Cas13 which was confirmed by the absence of viral DNA in qPCR (Fig. 4f).

To assess lateral-flow signal variability over time, we tested the same ten BKV positive or negative patient samples on three different days (Figs. 4g,h). We observed that all BKV negative samples were consistently below the band intensity cut-off on the three different days, whereas all BKV positive samples were above. This suggested a low variability of background noise and band intensities.

We also assessed the influence of incubation time and temperature on lateral-flow band intensity for two different concentrations of the CMV synthetic standard. For the negative control, the relative band intensity stayed below the 0.5 cut-off regardless of the incubation time, similar to our previous results (Supplementary Figs. 4a,b). When detecting 5 or 500 aM of CMV synthetic DNA, we observed a time-dependent increase of band intensities. Importantly, we could observe band intensity values above the cut-off only after 60 min, indicating that our assay incubation time could be further shortened. For different reaction temperatures ranging from 21°C to 39°C, we again observed band intensity ratios below 0.5 for the negative control (Supplementary Figs. 4c,d). While room temperature (21°C) was sufficient to detect 5 and 500 aM of CMV synthetic standard, higher temperatures correlated with higher band intensities. These results indicate that reaction time and temperature are important variables if a quantitative lateral flow read-out is the goal. In contrast, highly consistent background noise irrespective of daily variation, incubation time and temperature enables a robust qualitative assay.

We further optimized the combination of RPA, T7 transcription and Cas13 in one reaction ("one-pot reaction", Supplementary Fig. 5a) by testing different reaction buffers and nucleotide ratios (Supplementary Figs. 5b-d). Using this optimized one-pot reaction, we achieved BKV detection in the atto-molar range (Supplementary Fig. 5e).

Detection of *CXCL9* mRNA levels with lateral-flow enables monitoring of kidney rejection and treatment response

Next, we sought to apply the lateral-flow-based assay for the detection of *CXCL9* mRNA indicative of acute cellular kidney rejection. Similar to the detection of viral DNA, lateral flow enabled robust detection of *CXCL9* synthetic RNA (Fig. 5a) down to the atto-molar range. Using nonlinear regression analysis, we determined that a concentration of 12 aM corresponded to the 0.5 band intensity cut-off.

In order to explore the power of our CRISPR-based read-out for rejection monitoring, we selected two patients experiencing allograft cellular rejection as confirmed by biopsy who had at least three prospective samples after the rejection event (Figs. 5b,c). Patient 1 (Fig. 5b) developed an acute cellular rejection (Banff IIA) and showed a good response to treatment with thymoglobulin and pulse methylprednisolone, achieving full clinical recovery. This was reflected by a strong downregulation of *CXCL9* mRNA levels as observed in qPCR and return to his baseline serum creatinine (0.9 mg/dL). CRISPR-based testing detected *CXCL9* mRNA only during rejection, while the patient was *CXCL9* negative after treatment completion.

In contrast, Patient 2 (Fig. 5c) had an episode of acute cellular rejection Banff IIA with partial improvement of creatinine after treatment (Serum creatinine 3.5 mg/dL down from 7.9). While urine *CXCL9* mRNA was reduced initially, it went back up 7 months afterwards, and repeat biopsy revealed chronic active cellular rejection. Overall, monitoring of urine *CXCL9* mRNA levels may be a useful tool to assess response to rejection treatment, though further validation in a larger trial is needed.

Discussion

Fast and cost-effective POCT should enable early diagnosis and greater accessibility for patients in low-resource settings, including the opportunity for self-monitoring. Here, we applied CRISPR-Cas13 diagnostics to detect CMV and BKV infection in samples of kidney transplant patients. We extended the use of SHERLOCK for the detection of *CXCL9* mRNA, a biomarker of acute cellular rejection of kidney transplants. Together, these developments may enable the cost-effective (Supplementary Table S3) monitoring of patients at risk for opportunistic infection and serve as a tool for earlier detection of rejection and monitoring post-treatment in transplantation.

BKV and CMV are among the most common opportunistic infections after solid-organ transplantation, being associated with significant morbidity[21]. However, clinical presentation is variable in transplanted patients and BKV infection frequently presents without clinical symptoms except a creatinine rise, which indicates already established BK nephropathy. Blood testing for BKV and CMV viral load is recommended but not uniformly performed in all centers due to cost limitations, in particular in developing countries. Here, our high-sensitivity, low-cost POC assay could allow for more frequent testing.

Rejection is the leading cause of chronic allograft loss. However, rejection is usually detected late since serum creatinine is a delayed marker of allograft injury. Furthermore, the diagnosis of acute rejection currently requires a renal biopsy - an invasive process that is limited by sampling error and assessment variability[22]. In order to detect graft injury earlier, some centers perform surveillance kidney biopsies at pre-specified time-points post-transplant[23]. However, these procedures are associated with major risks for patients, such as bleeding, and significant costs (~$3,500/biopsy, which includes the procedure and the pathological analyses of the kidney specimen). Therefore, a sensitive and non-invasive assay such as CRISPR-Cas13-based *CXCL9* mRNA testing could allow for more frequent testing and thereby achieve earlier detection of graft rejection, allowing timely diagnosis and treatment.

Here, we focused on cellular-mediated rejection, the most frequent rejection affecting kidney transplant patients. Screening for donor-specific anti-HLA antibodies (DSA) is currently performed in patients with concern for antibody-mediated rejection. All patients included in our study had a negative test for DSA. Screening prospectively for DSA in all patients is not uniformly performed in part due to lack of specificity of DSA to antibody-mediated rejection[24,25]*.*

Two novel blood tests that detect the fraction of donor-derived cell-free DNA have become clinically available in kidney transplantation to monitor for rejection[26,27]. While these assays have shown promising results, they still require a visit to the clinic to draw blood, shipping of the material to outside labs for processing and analysis, and they have a high price tag of US $2,821 per test[28]. This high price limits the frequency of testing and also prevents the use of this test in resource-limited settings. The advantages of our rejection assay are its low cost, its high sensitivity and its use of urine compared to blood. Since *CXCL9* mRNA elevation in the urine can be detected weeks before elevation of creatinine due to rejection[29], urine *CXCL9* mRNA monitoring may represent a promising technique for earlier rejection detection as well as post-treatment monitoring. Lastly, the development of a smartphone application to enable simple and fast interpretation of the lateral-flow assay allows for sharing of results directly with the provider, leading to a convenient way of monitoring patients between clinical appointments.

Our test was mainly aimed for the qualitative detection of CMV, BKV and *CXCL9* at clinically relevant concentrations. However, in many clinical situations, precise quantification of the viral

load and changes in biomarker levels are useful. Future iterations of this protocol should, therefore, include quantitation strategies and may build on recent protocols demonstrating semi-quantitative read-outs of CRISPR diagnostics[3]. This would also strengthen the power of CRISPR-based diagnostics, since it could allow for the detection of subtle changes as a deviation from an individualized baseline. Moreover, although most steps could be optimized for a POCT setting, sample isolation for the detection of mRNA still required a column-based approach. Thus, further work will consist in optimizing the protocol for simplified mRNA isolation procedures. In addition, heating represents an essential step in our current sample processing protocol using HUDSON. Thus, the integration of POC heating devices using chemical[30] or electromagnetic[31] heating might facilitate handling for the primary care provider or patient. Finally, inclusion of more patient samples and prospective analysis will allow for systematic comparison with current clinical practice.

In summary, this work demonstrates the application of CRISPR-Cas13 for the detection of rejection and opportunistic infection in kidney transplantation. This technology could be easily applied to other solid-organ transplants as well as immune-mediated kidney diseases such as lupus nephritis. Based on its low-cost, ease of use and speed, this assay could allow frequent testing and earlier diagnosis. The next steps in order to advance clinical implementation include studies to validate these findings and to demonstrate the clinical utility of this assay in regard to long-term outcomes of kidney transplant recipients.

Methods

Lateral flow reactions. 20µl of the Sherlock reaction containing the lateral flow reporter-oligo at 1µM (sequence in supplementary table 4) were mixed with 80µl of Hybridetect Assay buffer, followed by insertion of lateral flow-sticks (Milenia Hybridetect1, TwistDx Limited, Maidenhead, UK) and incubation for 3min at room temperature, according to the manufacturer's instructions, before images were taken.

Image analysis of lateral flow reactions. The relative band intensities of each of the lateral-flow sticks were measured using ImageJ software (US National Institute of Health). The relative band intensity was calculated as the test band's mean grey value/control band's mean grey value. Images were first converted to 8-bit and inverted, before highlighting the band region and measuring its mean grey value.

Lateral flow quantification app. The lateral flow quantification algorithm was implemented using Python's opencv package (v4.1.1). Briefly, images uploaded to the app are automatically

converted to grayscale and the colors are inverted. The resultant image is then subjected to a Gaussian blur in order to remove outlier pixels that may result in artifactual bright-spots. Afterward, a threshold is applied to accentuate bright spots. Connected component analysis is then used to isolate regions corresponding to the control and sample bands. These bands are then identified and quantified by calculating the mean intensity of each band. If the sample band cannot be identified due to weak intensity, the sample band's location is estimated by scanning for bright areas in the upper portion of the lateral flow stick using the control band as a perspective scale. The ratio of the sample to control band is then calculated and displayed to the user. The Android app was developed with Android Studio v3.5.1 (Google, Mountain View, CA) with Java 8 and Gradle v5.4.1 (Supplementary Video 1). To provide a clean user interface, the main screen was limited to three buttons: (1) upload new pictures, (2) specify the target of the assay (i.e., CMV, BKV, or CXCL9), and (3) initiate image analysis. The picture upload process requests read permissions of the phone's photo gallery. Image analysis allows for two options, with the faster analysis scaling down the image to 50% lower resolution for more rapid results. The pixel array is passed to a Python backend through Chaquopy v6.3.0, a Python SDK for Android.

Sample preparation. Patient samples containing CMV or BKV were prepared as indicated, either with the previously described HUDSON protocol[2] or the QIAamp MinElute Virus Spin Kit (Qiagen, Hilden, Germany), according to the manufacturer's instructions. For HUDSON processing, the samples were heated for 10min at 95°C in the presence of 100mM TCEP (Fisher Scientific, USA) and 1mM EDTA (Fisher Scientific, USA). For *CXCL9* mRNA detection, 45 ml urine was centrifuged for 30min at 2000g at 4°C, followed by washing of the pellet with PBS and resuspension in 200µl RNAlater (Qiagen, Hilden, Germany). All samples were aliquoted and stored at -80°C. RNA was isolated using the RNeasy Micro Kit (Qiagen, Hilden, Germany) and the PureLink RNA Mini Kit (Invitrogen, USA), following the manufacturer's instructions.

Production of crRNAs and LwaCas13a. LwaCas13a was produced by Genscript (Piscataway, USA). crRNAs were synthesized using the HiScribe™ T7 Quick High Yield RNA Synthesis Kit (NEB, Ipswich, USA), according to the manufacturer's instructions, with the T7 promoter containing annealed oligonucleotides. Reactions were incubated for 16h at 37°C, DNAse (NEB) digested and purified using the RNA Clean & Concentrator-25 kit (ZymoResearch, Irvine, USA).

RPA primer and crRNA design. Genetically conserved regions in the BKV and CMV genome were identified using publicly accessible databases (Virus Pathogen Resource and NCBI). Alignments were performed using MAFFT[32] and visualized with Jalview[33]. RPA primer design

was done using NCBI's PRIMER-BLAST tool with previously described settings[3]. *CXCL9* RPA primers were designed to be in proximity to previously published qPCR primers[18]. For each region to be amplified, optimal primer pairs were identified by forward and reverse primer screens. Primer concentrations were optimized by testing different forward and reverse primer concentrations in a dilution matrix. crRNAs, 28 nucleotides complementary to the target region, were designed as previously described[1,3] and tested for their performance with each RPA primer pair. The sequences, including spacer, direct repeat and T7 promoter, are indicated in Supplementary Table 4.

qRT-PCR. RNA isolation, reverse transcription and qPCR were performed as previously described[18]. Briefly, we reverse transcribed RNA using the TaqMan Reverse Transcription kit (ThermoFisher, Waltham, USA) with random hexamers. The qPCR was performed using cDNA without pre-amplification. qPCR reactions were set up as previously described[18]. All reactions were performed in duplicate, using the Applied Biosystems StepOne Plus real-time PCR system (ThermoFisher, Waltham, USA). In-vitro transcribed RNA for *CXCL9* served as a standard (sequences in Supplementary Table 4). For expression analysis, we employed the comparative C_T method[34] for relative quantification to 18S RNA (Supplementary Figure 3a) or used absolute quantification based on a *CXCL9* standard curve (Figures 5b,c). Expression levels are presented on a logarithmic scale relative to the control, whose average expression was set to 1.

RPA reactions. For RPA reactions, the TwistAmp Liquid Basic kit (TwistDx Limited, Maidenhead, UK) was used according to the manufacturer's instructions with the following modifications. Primer concentrations were 120nM for the forward primer and 480nM for the reverse primer. The total reaction volume was 20µl with a final concentration of dNTPs at 7.2mM (each) and MgOAc at 8mM. RPA reactions were incubated at 37°C for 50min. For rt-RPA reactions, forward and reverse primers were used at 480nM each and MgOAc at 14mM. 1µl GoScript reverse transcriptase (Promega) was added to a 20µl reaction containing DL-Dithiothreitol solution (DTT, Sigma-Aldrich) at a final concentration of 19mM. The primer-RNA mix was pre-incubated at 65°C for 10min and the rt-RPA reaction was performed at 42°C for 60min.

Cas13 reactions. Detection of (rt)RPA amplified targets was performed as described previously[1–3] with minor modifications. NEB buffer 2 (NEB, Ipswich, USA) served as cleavage buffer at a final concentration of 1X. 3µl of RPA or rtRPA product were used in a 20µl Cas13 reaction. Fluorescence (485nm excitation, 520nm emission) was measured on a plate reader (SpectraMax M5, Molecular Devices, San Jose, USA) every 5min for up to 3h at 37°C.

One-pot reaction. One pot RPA-CRISPR reactions were performed with murine RNAse Inhibitor (NEB) at 1U/µl, Cas13 at 45nM, crRNA at 22.5nM, RNAse Alert V2 (Thermofisher) at 125nM, human background RNA (from 293T cells) at 1.25ng/µl, T7 polymerase (Lucigen) at 0.6µl/20µl, dNTPs at 1.8mM (each), rNTPs at 0.5mM (each), MgOAc at 16mM and the buffers of the RPA TwistAmp Liquid Basic kit (2X, 10X and 20X buffers) at 1X final concentrations.

Diagnostic BKV and CMV quantitative PCR. De-identified patient samples were provided by the Crimson Core at Brigham and Women's Hospital. Quantification of BKV and CMV viral load were performed at the CLIA certified diagnostic core facility at Brigham and Women's Hospital. In brief, BKV viral load samples were processed using the Luminex Aries instrument (Luminex, Austin, USA) and a laboratory-developed protocol for a probe-free, two-primer, real-time PCR system. Following amplification, a thermal melt was performed. The system software allows for a quantitation template, developed using a standard curve calibrated against the 1st WHO International Standard for BKV, to be applied to raw data for production of a quantitative value, reported in copies/mL (C/mL). CMV viral load samples were processed using the Roche Cobas AmpliPrep/Cobas TaqMan CMV Test (IVD) on the Roche-docked Cobas AmpliPrep/TaqMan instrument. This is a real time PCR system that automates specimen preparation, PCR amplification, target detection and quantitation. Results are reported in International Units/mL (IU/mL).

Patient populations. For the CMV and BK studies, de-identified samples collected for clinical testing for CMV and BK viremia at the Brigham and Women's Hospital (BWH) were provided by the Crimson Core at BWH. Clinical reported results for CMV and BK viremia were then compared to CRISPR/Cas13 diagnostics results. For the rejection and BK nephropathy samples, patients were recruited prior to a kidney transplant biopsy to investigate an elevation of creatinine at BWH. Prospective sample collection was also performed in few kidney transplant recipients starting in January 2019 until June 2019. Samples started to be collected after one month of transplantation to avoid the impact of surgery and ischemic time. Samples were then collected according to clinical visits for 3-5 collections within the first year of transplant. The kidney transplant cohort is representative of kidney transplant recipients in this geographical location and at a tertiary academic hospital.

Study design and participants. The study was approved by the Institutional Review Board at Brigham and Women's Hospital (2017P000298), and the procedures followed were in accordance with institutional guidelines. In this observational study, a total of 31 kidney transplant patients were enrolled, and informed consent was obtained from all subjects (Supplementary Tables 1,2). Urine samples were collected from patients undergoing kidney

biopsy for clinical indications. The cohort of samples was then selected based on the presence of cellular rejection or no rejection on biopsy findings. For the prospective analyzes, samples were provided by a cohort from Montefiore Medical Center, Bronx, NY (Montefiore/Einstein Institutional Review Board (09-06-174). Briefly, longitudinal samples were collected at the following time points: 0-3 months, 6-9 months and 9-12 months post-transplant or when clinical biopsy was performed). Selection of patients was based on availability of at least three samples collected either before or after rejection event that was classified as rejection Banff IA or higher.

Ethics statement. We have complied with all relevant ethical regulations. The patient samples used in this study were obtained from the clinical study "*Biomarkers in Kidney Transplantation*" which was approved by Partners Human Research Committee (2017P000298/PHS). We have obtained written informed consent from all participants.

Data availability statement. The authors declare that the data supporting the findings of this study are available within the paper and its supplementary information files.

Code availability statement. The lateral flow quantification app code is available at https://github.com/jackievaleri/lateral_flow_quantification_app.

References

1. Gootenberg, J. S. *et al.* Nucleic acid detection with CRISPR-Cas13a/C2c2. *Science (80-.).* **356**, 438–442 (2017).
2. Myhrvold, C. *et al.* Field-deployable viral diagnostics using CRISPR-Cas13. *Science (80-.).* **448**, 444–448 (2018).
3. Gootenberg, J. S. *et al.* Multiplexed and portable nucleic acid detection platform with Cas13, Cas12a, and Csm6. *Science (80-.).* **0179**, (2018).
4. Chen, J. S. *et al.* CRISPR-Cas12a target binding unleashes indiscriminate single-stranded DNase activity. *Science* **360**, 436–439 (2018).
5. Harrington, L. B. *et al.* Programmed DNA destruction by miniature CRISPR-Cas14 enzymes. *Science (80-.).* **362**, 839 LP – 842 (2018).
6. Pardee, K. *et al.* Rapid, Low-Cost Detection of Zika Virus Using Programmable Biomolecular Components. *Cell* **165**, 1255–1266 (2016).
7. Hajian, R. *et al.* Detection of unamplified target genes via CRISPR–Cas9 immobilized on a graphene field-effect transistor. *Nat. Biomed. Eng.* **3**, (2019).
8. Wu, Y., Liu, S.-X., Wang, F. & Zeng, M.-S. Room Temperature Detection of Plasma Epstein–Barr Virus DNA with CRISPR–Cas13. *Clin. Chem.* **65**, 591 LP – 592 (2019).
9. Lamb, K. E., Lodhi, S. & Meier-Kriesche, H.-U. Long-Term Renal Allograft Survival in the United States: A Critical Reappraisal. *Am. J. Transplant.* **11**, 450–462 (2011).
10. Tullius, S. G. & Rabb, H. Improving the Supply and Quality of Deceased-Donor Organs for

Transplantation. *N. Engl. J. Med.* **378**, 1920–1929 (2018).
11. Wekerle, T., Segev, D., Lechler, R. & Oberbauer, R. Strategies for long-term preservation of kidney graft function. *Lancet* **389**, 2152–2162 (2017).
12. Ross, S. A., Novak, Z., Pati, S. & Boppana, S. B. Overview of the diagnosis of cytomegalovirus infection. *Infect. Disord. Drug Targets* **11**, 466–474 (2011).
13. Randhawa, P. *et al.* Correlates of quantitative measurement of BK polyomavirus (BKV) DNA with clinical course of BKV infection in renal transplant patients. *J. Clin. Microbiol.* **42**, 1176–1180 (2004).
14. Fishman, J. A. Infection in Organ Transplantation. *Am. J. Transplant.* **17**, 856–879 (2017).
15. Sepkowitz, K. A. Opportunistic Infections in Patients with and Patients without Acquired Immunodeficiency Syndrome. *Clin. Infect. Dis.* **34**, 1098–1107 (2002).
16. Sundsfjord, A. *et al.* BK and JC Viruses in Human Immunodeficiency Virus Type 1-Infected Persons: Prevalence, Excretion, Viremia, and Viral Regulatory Regions. *J. Infect. Dis.* **169**, 485–490 (1994).
17. Jackson, J. A. *et al.* Urinary chemokines CXCL9 and CXCL10 are noninvasive markers of renal allograft rejection and BK viral infection. *Am. J. Transplant.* **11**, 2228–2234 (2011).
18. Hricik, D. E. *et al.* Multicenter validation of urinary CXCL9 as a risk-stratifying biomarker for kidney transplant injury. *Am. J. Transplant.* (2013) doi:10.1111/ajt.12426.
19. Schaub, S. *et al.* Urinary CXCL9 and CXCL10 levels correlate with the extent of subclinical tubulitis. *Am. J. Transplant.* **9**, 1347–1353 (2009).
20. Rabant, M. *et al.* Early Low Urinary CXCL9 and CXCL10 Might Predict Immunological Quiescence in Clinically and Histologically Stable Kidney Recipients. *Am. J. Transplant.* **16**, 1868–1881 (2016).
21. Fishman, J. A. Infection in Solid-Organ Transplant Recipients. *N. Engl. J. Med.* **357**, 2601–2614 (2007).
22. El-Zoghby, Z. M. *et al.* Identifying specific causes of kidney allograft loss. *Am. J. Transplant* **9**, 527–535 (2009).
23. Henderson, L. K., Nankivell, B. J. & Chapman, J. R. Surveillance protocol kidney transplant biopsies: their evolving role in clinical practice. *Am. J. Transplant* **11**, 1570–1575 (2011).
24. Parajuli, S. *et al.* Donor-Specific Antibodies in the Absence of Rejection Are Not a Risk Factor for Allograft Failure. *Kidney Int. reports* **4**, 1057–1065 (2019).
25. Schinstock, C. A. *et al.* The Value of Protocol Biopsies to Identify Patients With De Novo Donor-Specific Antibody at High Risk for Allograft Loss. *Am. J. Transplant* **17**, 1574–1584 (2017).
26. Bloom, R. D. *et al.* Cell-Free DNA and Active Rejection in Kidney Allografts. *J. Am. Soc. Nephrol.* **28**, 2221–2232 (2017).
27. Sigdel, T. K. *et al.* Optimizing Detection of Kidney Transplant Injury by Assessment of Donor-Derived Cell-Free DNA via Massively Multiplex PCR. *J. Clin. Med.* **8**, (2018).
28. UNITED STATES SECURITIES AND EXCHANGE COMMISSION.

https://www.sec.gov/Archives/edgar/data/1217234/000156459018006584/cdna-10k_20171231.htm.
29. Hricik, D. E. *et al.* Adverse Outcomes of Tacrolimus Withdrawal in Immune–Quiescent Kidney Transplant Recipients. *J. Am. Soc. Nephrol.* **26**, 3114–3122 (2015).
30. Curtis, K. A. *et al.* Isothermal Amplification Using a Chemical Heating Device for Point-of-Care Detection of HIV-1. *PLoS One* **7**, e31432 (2012).
31. Ahn, M.-H., Baek, S.-K., Min, J. & Park, J.-H. A portable electromagnetic induction heating device for point-of-care diagnostics. *BioChip J.* **10**, 208–214 (2016).
32. Katoh, K. & Standley, D. M. MAFFT multiple sequence alignment software version 7: improvements in performance and usability. *Mol. Biol. Evol.* **30**, 772–780 (2013).
33. Waterhouse, A. M., Procter, J. B., Martin, D. M. A., Clamp, M. & Barton, G. J. Jalview Version 2—a multiple sequence alignment editor and analysis workbench. *Bioinformatics* **25**, 1189–1191 (2009).
34. Schmittgen, T. D. & Livak, K. J. Analyzing real-time PCR data by the comparative CT method. *Nat. Protoc.* **3**, 1101 (2008).

Acknowledgments

We thank Rebecca Zaffini from viral microbiology (Brigham & Women's Hospital) for helpful discussion about BKV testing and qPCR. We thank the Crimson Core at Brigham & Women's Hospital for providing CMV and BKV patient samples. M.M.K was supported by the German Academy of Sciences, Leopoldina (LPDS 2018-01) and the Clinician Scientist Program Berta-Ottenstein of the Faculty of Medicine, University of Freiburg, Germany. M.A.A was supported by a National Science Foundation graduate research fellowship (1122374). V.K. was supported by the DFG (403877094). J.J.C. was supported by MIT's Center for Microbiome Informatics and Therapeutics, the Paul G. Allen Frontiers Group, and the Wyss Institute. We thank Helena de Puig, Nicolaas Angenent-Mari, Aaron Dy and Xiao Tan for helpful discussions.

Author contributions

M.M.K., L.V.R. and J.J.C. designed the study. M.M.K., M.A.A., A.C.H., I.L. and R.G. performed experiments. J.V. and M.A.A. programmed the smartphone app, L.V.R. provided clinical samples. All authors contributed to the writing of the manuscript and interpretation of data.

Competing interests

A patent application is pending. J.J.C is co-founder and director of Sherlock Biosciences.

Figure 1

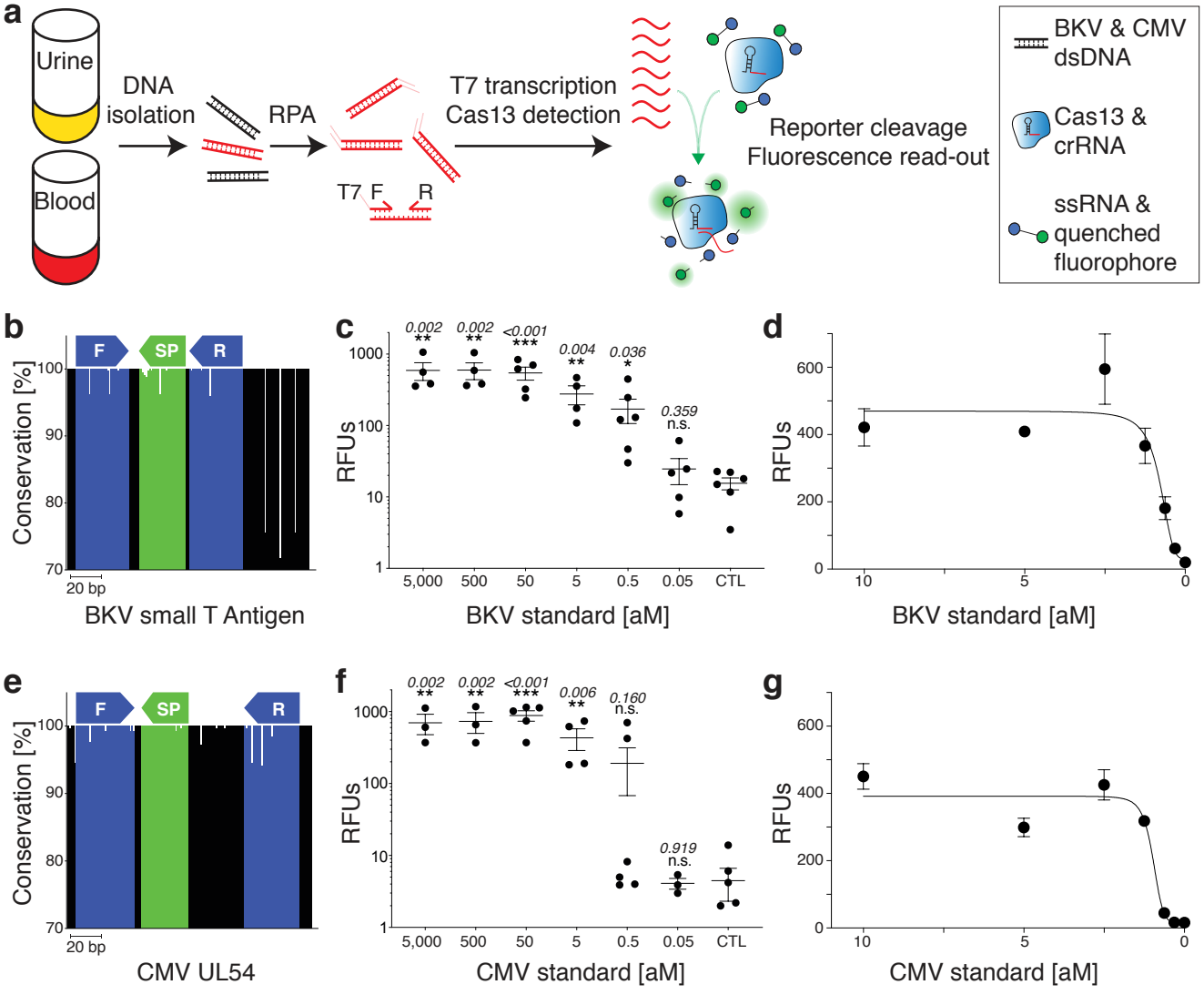
a
Urine
Blood
DNA isolation
RPA
T7 F R
T7 transcription
Cas13 detection
Reporter cleavage
Fluorescence read-out
BKV & CMV dsDNA
Cas13 & crRNA
ssRNA & quenched fluorophore
b
F
SP
R
Conservation [%]
20 bp
BKV small T Antigen
c
RFUs
0.002
0.002
<0.001
0.004
0.036
0.359
n.s.
5,000
500
50
5
0.5
0.05
CTL
BKV standard [aM]
d
RFUs
BKV standard [aM]
e
CMV UL54
f
0.002
0.002
<0.001
0.006
0.160
n.s.
0.919
n.s.
CMV standard [aM]
g
CMV standard [aM]

Figure 2

a

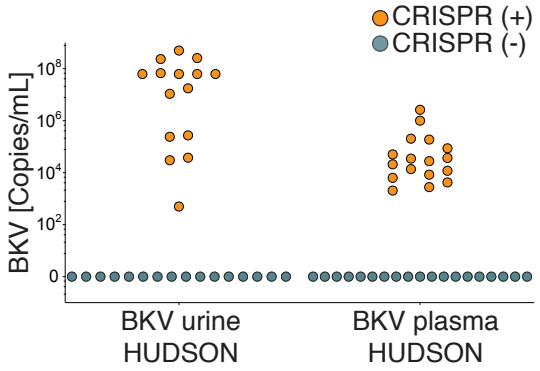

b

	VIRUS (+)	VIRUS (-)
CRISPR (+)	**True positive**	False positive
CRISPR (-)	False negative	**True negative**
	Sensitivity	*Specificity*

BKV urine HUDSON

15	0
0	**16**

100% 100%

BKV plasma HUDSON

17	0
0	**19**

100% 100%

c

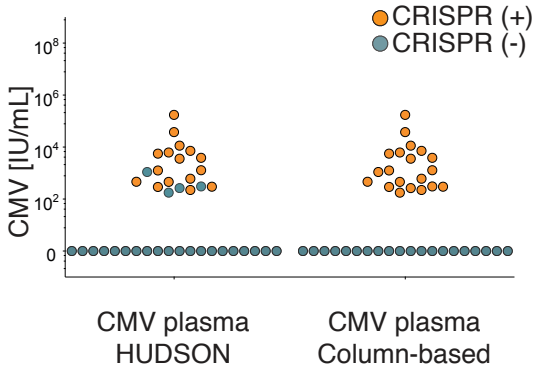

d

CMV plasma HUDSON

16	0
4	**20**

80% 100%

CMV plasma column-based

20	0
0	**20**

100% 100%

Figure 3

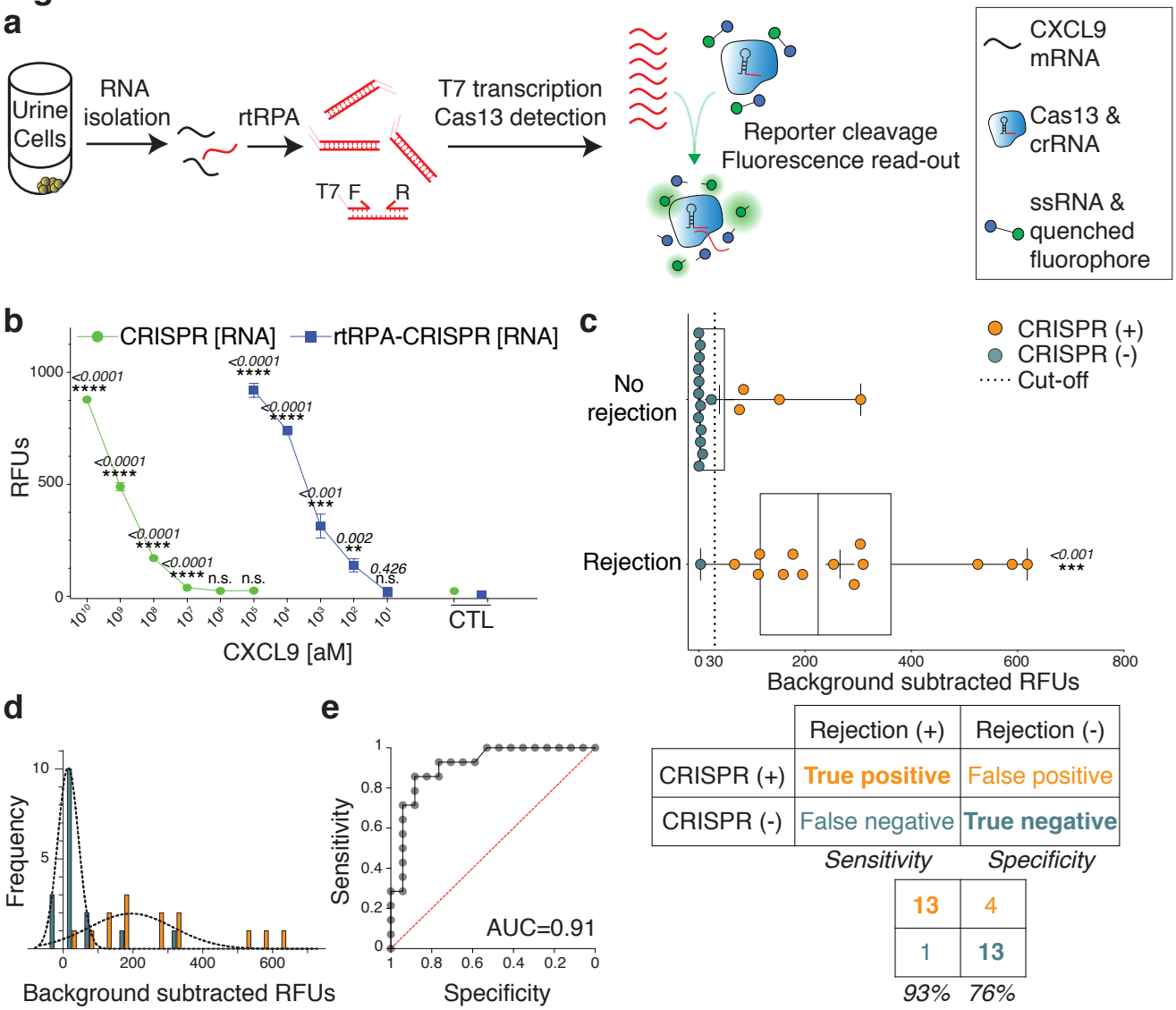

	Rejection (+)	Rejection (-)
CRISPR (+)	**True positive**	False positive
CRISPR (-)	False negative	**True negative**

Sensitivity *Specificity*

13	4
1	**13**

93% *76%*

Figure 4

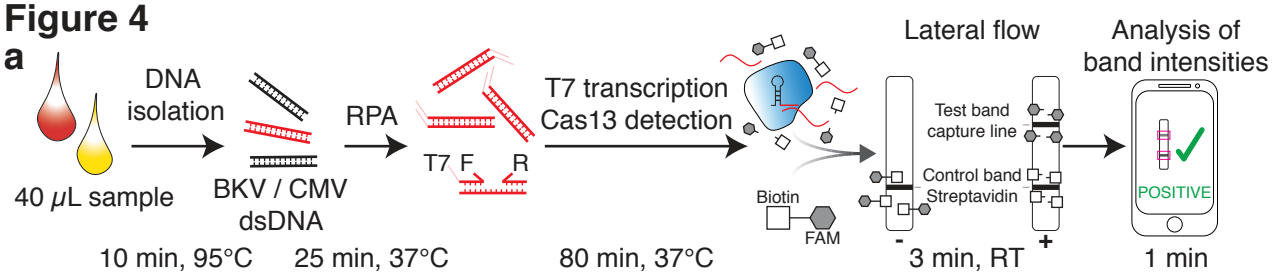
a
DNA isolation
RPA
T7 transcription Cas13 detection
Lateral flow
Analysis of band intensities
40 µL sample
BKV / CMV dsDNA
T7 F R
Biotin
FAM
Test band capture line
Control band Streptavidin
POSITIVE
10 min, 95°C
25 min, 37°C
80 min, 37°C
3 min, RT
1 min

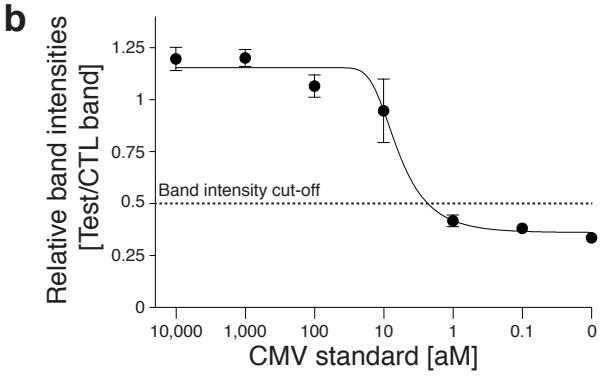
b
Relative band intensities [Test/CTL band]
Band intensity cut-off
CMV standard [aM]

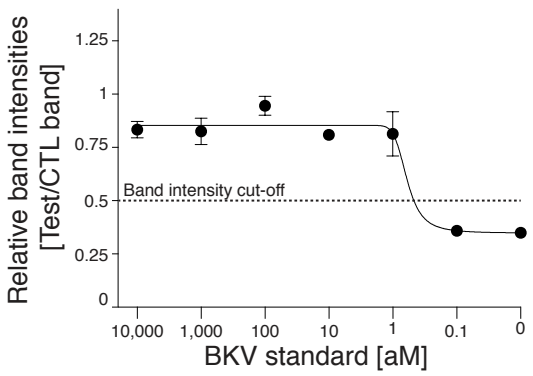
c
Relative band intensities [Test/CTL band]
Band intensity cut-off
BKV standard [aM]

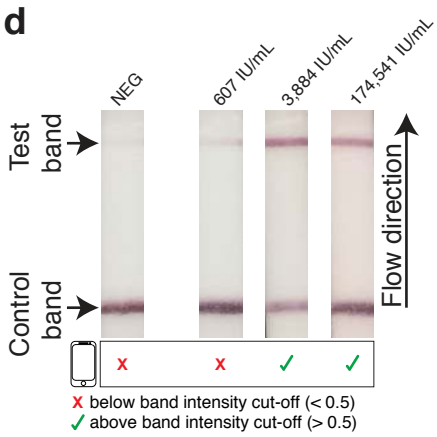
d
NEG
607 IU/mL
3,884 IU/mL
174,541 IU/mL
Test band
Control band
Flow direction
x below band intensity cut-off (< 0.5)
✓ above band intensity cut-off (> 0.5)

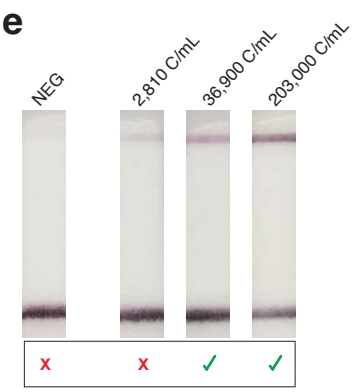
e
NEG
2,810 C/mL
36,900 C/mL
203,000 C/mL

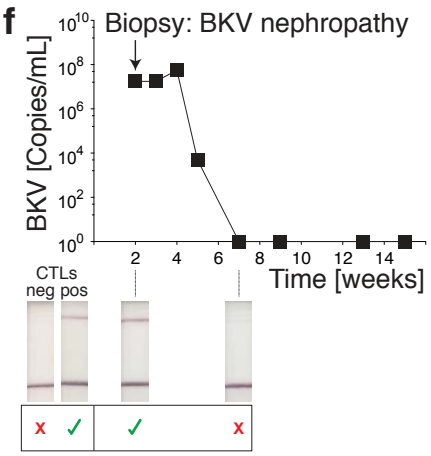
f
Biopsy: BKV nephropathy
BKV [Copies/mL]
Time [weeks]
CTLs neg pos

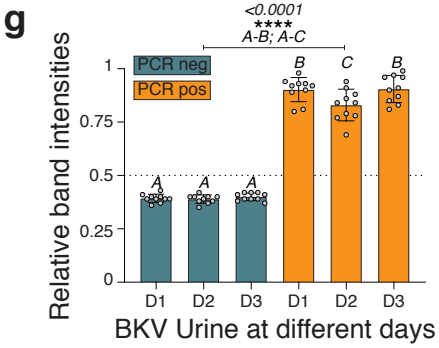
g
<0.0001
****
A-B; A-C
PCR neg
PCR pos
Relative band intensities
D1 D2 D3 D1 D2 D3
BKV Urine at different days

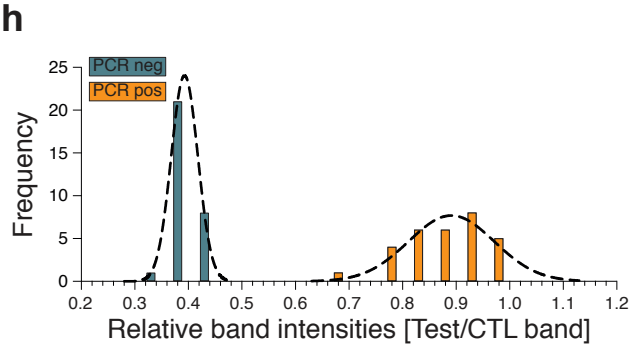
h
PCR neg
PCR pos
Frequency
Relative band intensities [Test/CTL band]

Figure 5

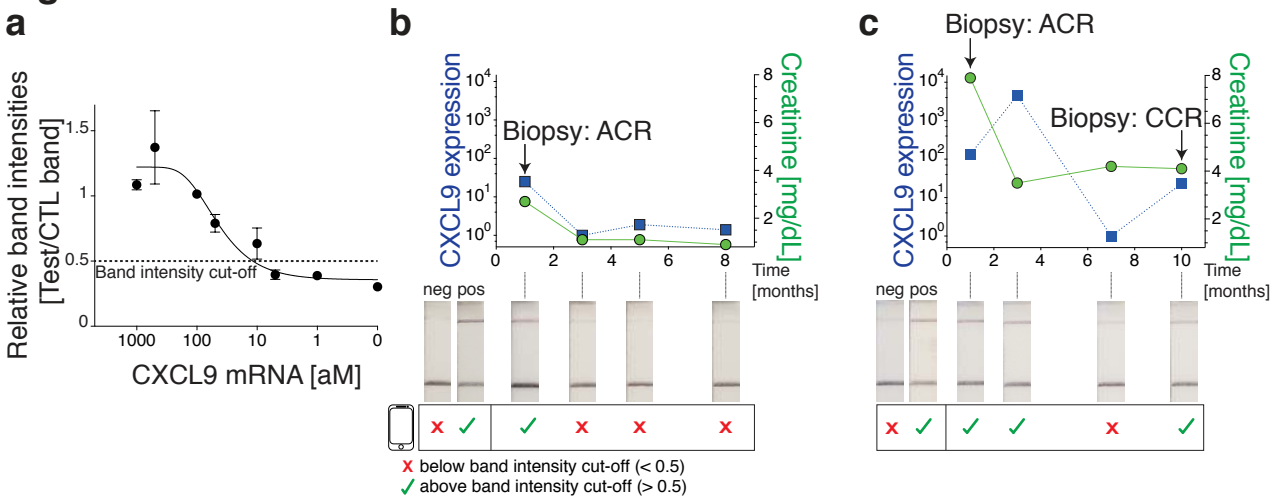
a
Relative band intensities [Test/CTL band]
1.5
1
0.5
0
Band intensity cut-off
1000
100
10
1
0
CXCL9 mRNA [aM]
b
CXCL9 expression
Biopsy: ACR
Creatinine [mg/dL]
Time [months]
neg pos
x ✓ ✓ x x x
x below band intensity cut-off (< 0.5)
✓ above band intensity cut-off (> 0.5)
c
Biopsy: ACR
Biopsy: CCR
CXCL9 expression
Creatinine [mg/dL]
Time [months]
neg pos
x ✓ ✓ ✓ x ✓

Supplementary Information

Contents:

Figure S1

a

BKV	CMV	Rejection marker
STA	UL54	CXCL9
VP2	UL55	CXCL10
VP3	UL83	
	UL97	

b

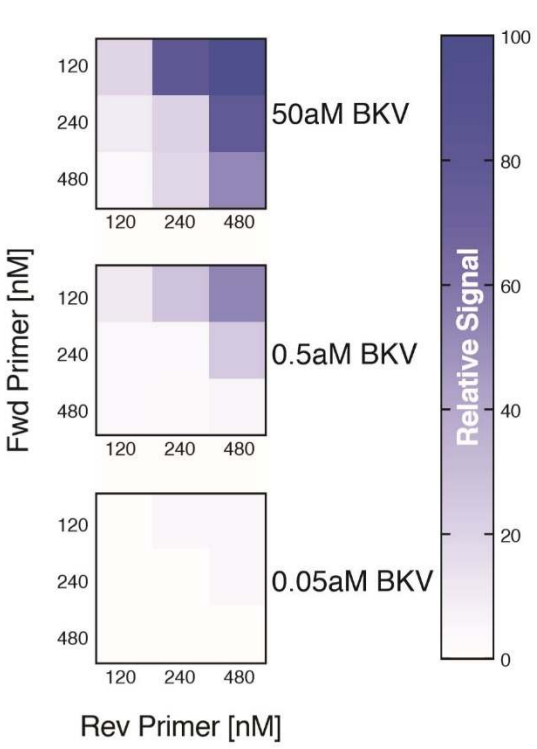

Supplementary Figure 1 Target genes and primer optimization. a, Target genes tested for detection of BKV or CMV infection and rejection. **b**, RPA primer dilution matrix. The Sherlock fluorescence signal of BKV detection (ATCC synthetic standard) at the indicated target concentrations is depicted as colour intensity relative to the highest signal (100). Forward and reverse primer concentrations for RPA as indicated.

Figure S2

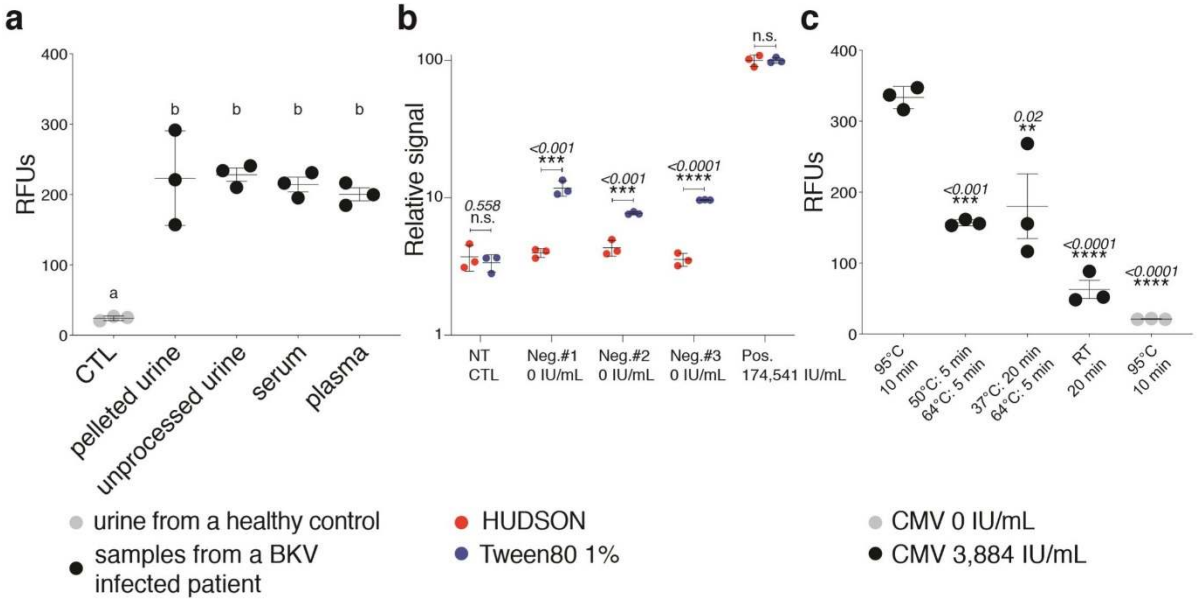

Supplementary Figure 2 Comparison of different specimen types and sample processing. a, Detection of BKV in the indicated specimens from the same patient compared to urine from a healthy control. Different small letters indicate significant differences as assessed by one-way ANOVA and Tukey's multiple comparisons test. Symbols: mean ± SD of 3 independent reactions. **b**, Comparison of sample processing by the HUDSON method (red circles) and incubation with Tween80 1% for 20 min at room temperature (blue circles). Tested on 3 different CMV negative patient samples to test for unspecific background noise and one CMV positive patient sample. Fluorescence was normalized to the highest signal (HUDSON, 100). Asterisks indicate significant differences as assessed by Student's two-tailed t-test. Symbols: mean ± SD of 3 independent reactions. **c**, Comparison of different HUDSON-based protocols on a CMV negative (grey circles) and a CMV positive (black circles) patient sample. Asterisks indicate significant differences to the 95°C/10 min (3884 IU/mL) condition as assessed by one-way ANOVA and Dunnett's multiple comparisons test. Symbols: mean ± SD of 3 independent reactions. n.s. not significant, $p<0.05$ (*), $p<0.01$ (**), $p<0.001$(***), $p<0.0001$ (****) (**b**,**c**).

Figure S3

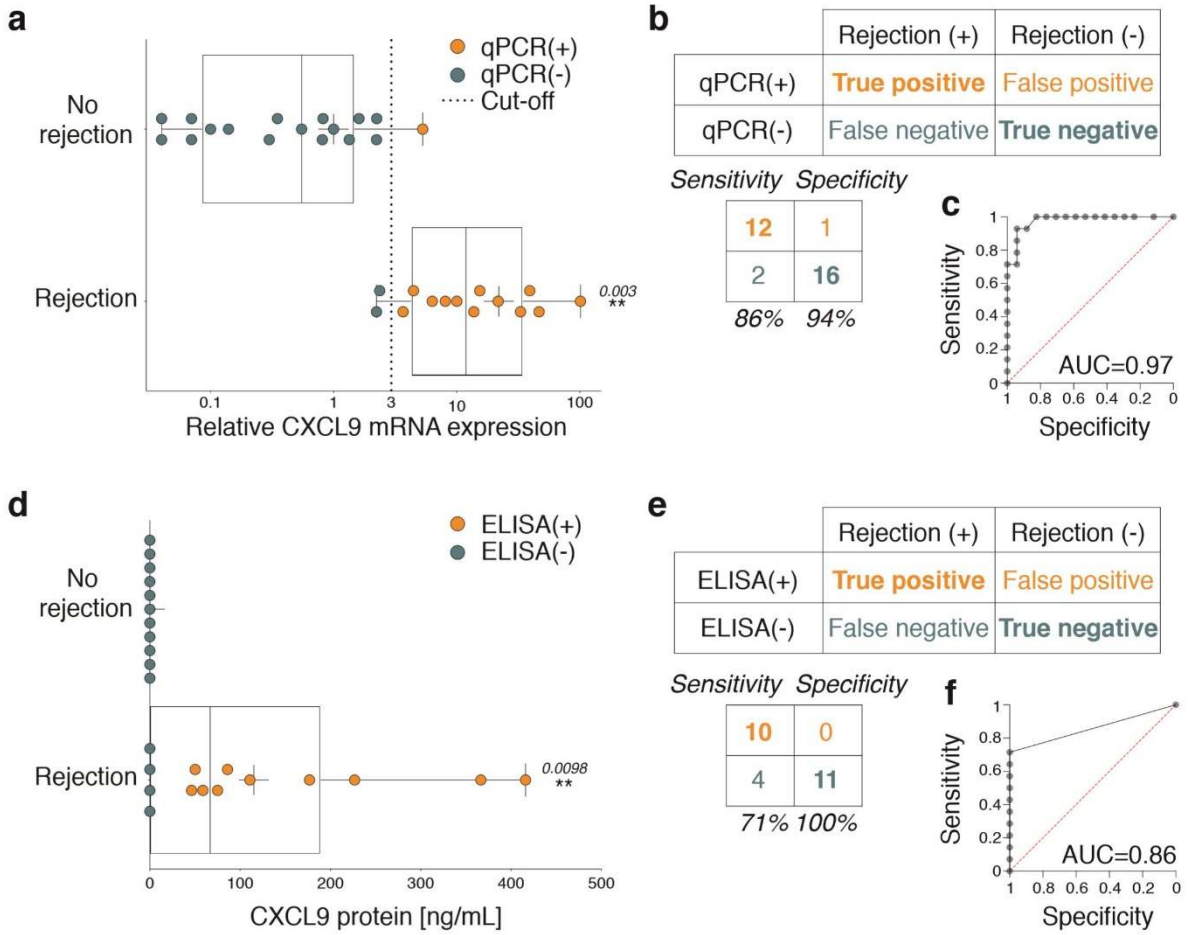

Supplementary Figure 3 CXCL9 mRNA and protein levels in rejection patients and controls. a, qPCR-based detection of CXCL9 mRNA in rejection patients (n=14) and no rejection control patients (n=17). Blue circles indicate qPCR negative tests and orange circles indicate qPCR positive test results. The dashed line indicates the cut-off differentiating between a negative and positive test result. **b**, Sensitivity and specificity of rejection detection by qPCR calculated using the cut-off value depicted in (a). **c**, Area under the receiver-operating-characteristic (ROC) curve (AUC) assessing the accuracy of qPCR-based rejection diagnostics (1 indicates perfect discriminatory value; 0.5 or less indicates no discriminatory value). **d**, ELISA-based detection of CXCL9 protein in rejection patients (n=14) and no rejection control patients (n=11). The tested samples were the same as depicted in (a) (rejection) or a subset of them (no rejection). Blue circles indicate ELISA negative tests and orange circles indicate ELISA positive test results. **e**, Confusion matrix indicating the sensitivity and specificity of ELISA-based rejection detection. **f**, Area under the receiver-operating-characteristic (ROC) curve (AUC) assessing the accuracy of ELISA-based rejection diagnostics (1 indicates perfect discriminatory value; 0.5 or less indicates no discriminatory value).

Box plot lines: median and quartiles, whiskers: data range, crosses: averages. Each symbol represents a different, independent patient sample. Asterisks: significant difference to control as assessed by Student's two-tailed t-test. $p<0.01$ (**) (**a**,**d**)

Figure S4

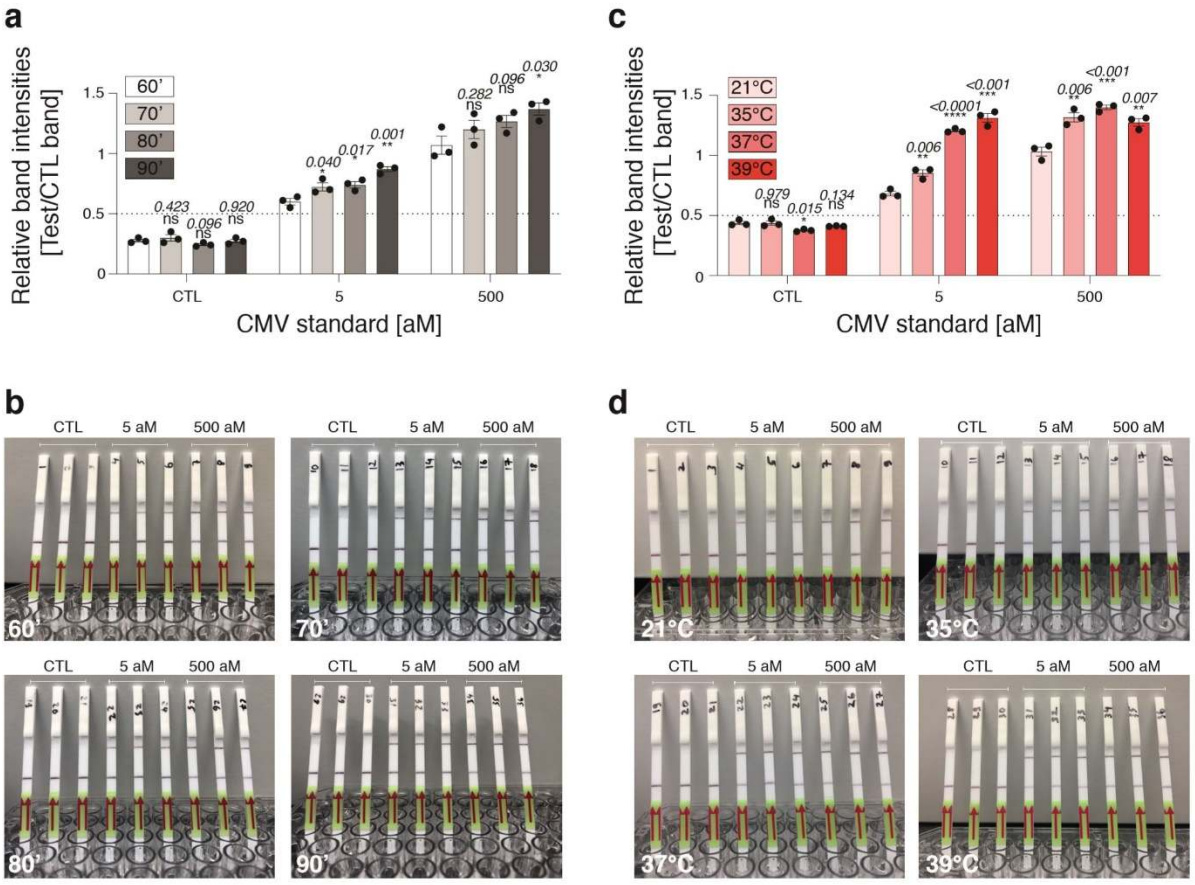

Supplementary Figure 4 Influence of temperature and incubation time on lateral-flow band intensity. a, Incubation of the CRISPR reaction detecting the CMV synthetic standard at the indicated concentrations for the indicated reaction times. The lateral-flow-based readout was quantified as the ratio of test/control band. The dashed line indicates the assay's cut-off. Symbols: mean ± SD of 3 independent reactions. Asterisks indicate significant differences to the 60 min control reaction time as assessed by Student's two-tailed t-test. **b**, Images of the lateral-flow assays quantified in (a). **c**, Incubation at different temperatures for the detection of the CMV synthetic standard at the indicated concentrations with lateral flow. Symbols: mean ± SD of 3 independent reactions. Asterisks indicate significant differences to the 21°C control reaction as assessed by Student's two-tailed t-test. **d**, Images of the lateral-flow assays quantified in (c). n.s. not significant, $p<0.05$(*), $p<0.01$ (**), $p<0.001$(***), $p<0.0001$ (****).

Figure S5

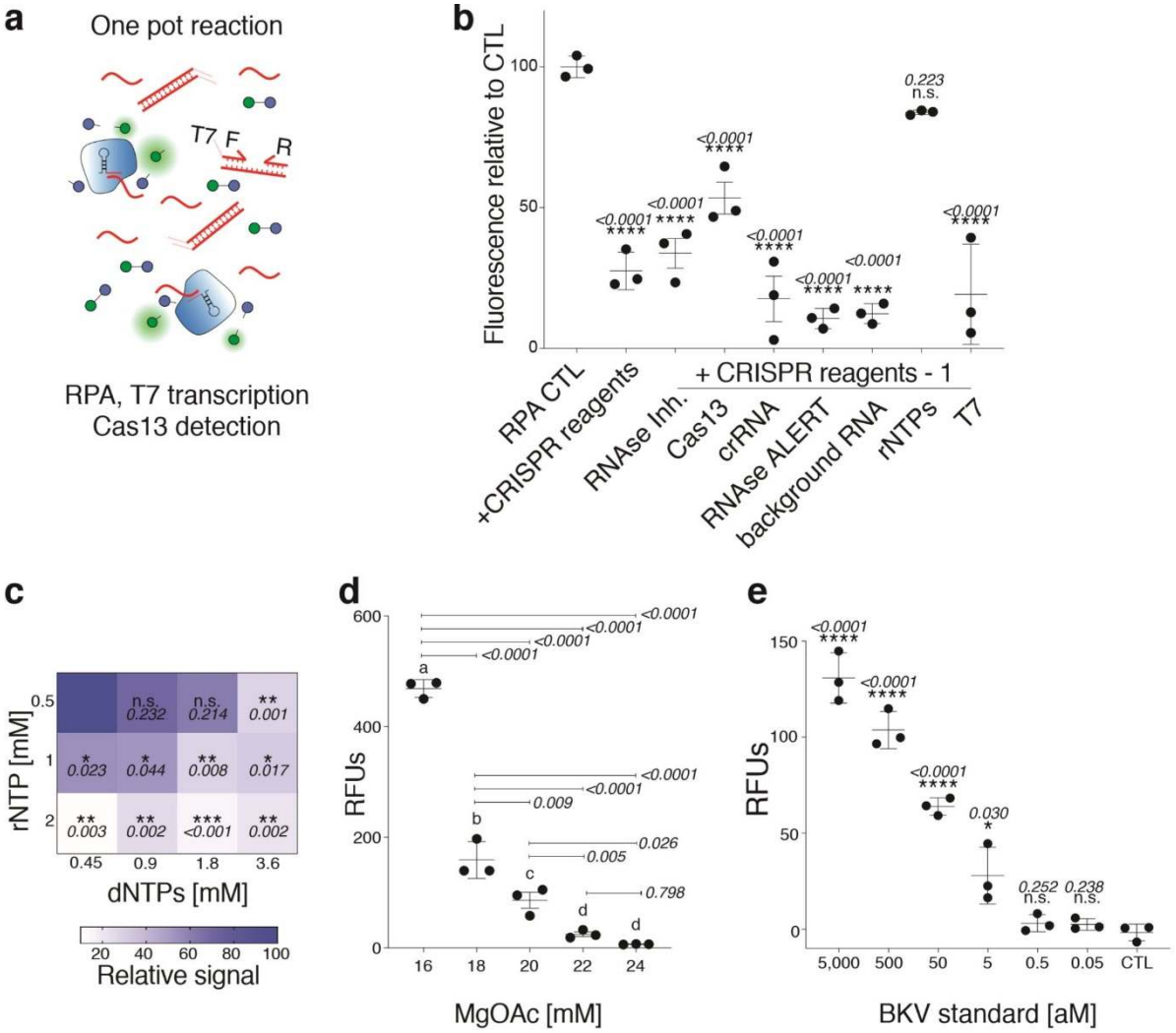

Supplementary Figure 5 Optimization of the one-pot reaction. a, Schematic illustration of the one-pot assay. **b**, Effect of CRISPR and T7 transcription reagents upon addition to the RPA reaction. CRISPR reagents were added pooled (+CRISPR reagents) or as a pool with one component missing (+CRISPR reagents -1). CMV synthetic DNA served as target (500aM). A separate CRISPR/T7 reaction served as readout. Fluorescence was normalized to the highest signal (RPA CTL, 100). Asterisks indicate significant differences to the RPA control without any additions (RPA CTL) as assessed by one-way ANOVA and Dunnett's multiple comparisons test. Symbols: mean ± SD of 3 independent reactions. **c**, Concentration matrix of rNTPs and dNTPs in the one-pot reaction. The fluorescence signal is depicted as colour intensity relative to the highest signal. Asterisks indicate significant differences as assessed by Student's two-tailed t-test. **d**, Testing of the indicated MgOAc concentrations in the one-pot reaction. CMV synthetic DNA served as target (500aM). Different letters indicate significant differences between groups as assessed by one-way ANOVA and Tukey's multiple comparisons test. Symbols: mean ± SD of 3 independent reactions. **e**, One-pot reaction detecting the ATCC quantitative BKV synthetic standard (Dunlop strain) at the indicated concentrations. Symbols: mean ± SD of 3 independent reactions. Asterisks indicate significant differences to no template control (CTL) as assessed by Student's two-tailed t-test. $p<0.05$ (*), $p<0.01$ (**), $p<0.001$(***), $p<0.0001$ (****).

Table S1

Characteristics	All subjects (N=31)	Rejection (n=14)	No Rejection (n=17)	p-value
Recipient Age (years)				
Mean ± SD	59 ± 13	61 ± 12	57 ± 14	0.589
Recipient Gender				
Female (n, %)	17 (54.8%)	5 (35.7%)	12 (70.6%)	0.076
Male (n, %)	14 (45.2%)	9 (64.3%)	5 (29.4%)	
Recipient Race				
African American (n, %)	10 (32.2%)	7 (50.0%)	3 (17.6%)	0.131
Caucasian (n, %)	14 (45.1%)	4 (28.6%)	10 (58.8%)	
Other / Unknown	7 (22.6%)	3 (21.4%)	4 (23.6%)	
Donor gender				
Female (n, %)	20 (64.5%)	9 (64.3%)	11 (64.7%)	0.999
Male (n, %)	11 (35.5%)	5 (35.7%)	6 (83.3%)	
Donor Source				
Living (n, %)	11 (35.5%)	4 (28.6%)	7 (41.2%)	0.707
Deceased (n, %)	20 (64.5%)	10 (71.4%)	10 (58.8%)	
Number of HLA mismatches				
Mean ± SD	4.4 ± 1.2	4.2 ± 0.9	4.6 ± 1.4	0.096
Induction Therapy				
Thymoglobulin (n, %)	16 (51.6%)	5 (35.7%)	11 (64.7%)	0.268
Basiliximab (n, %)	14 (45.2%)	8 (57.1%)	6 (35.3%)	
Alemtuzumab (n, %)	1 (3.2%)	1 (7.2%)	0 (0.0%)	
Time since transplant (months)				
Mean ± SD	12 ± 12	14 ± 13	11 ± 12	0.256
Cause of kidney disease				
Diabetes	7 (22.6%)	4 (28.5%)	3 (17.6%)	0.464
Polycystic kidney disease	5 (16.2%)	3 (21.5%)	2 (11.8%)	
Glomerulopathy	8 (25.8%)	3 (21.5%)	5 (29.5%)	
Interstitial Nephritis	3 (9.6%)	0 (0.0%)	3 (17.6%)	
Other/Unknown	8 (25.8%)	4 (28.5%)	4 (23.5%)	

Supplementary Table 1. Baseline and demographic characteristics of kidney transplanted patients. Baseline characteristics are presented as mean ± SD. For non-categorical variables, data were analysed using Mann-Whitney test. For categorical variables, data were analysed using Fisher's exact test.

Table S2

Characteristics	n=14
Creatinine (mg/dL)	3.24 ± 1.63
eGFR (ml/min/1.73m^2)	23.21 ± 9.27
Rejection Type (n, %)	
Borderline	1 (7.2%)
IA/IB	8 (57.1%)
IIA/IIB	4 (28.5%)
III	1 (7.2%)
Banff g score	1.5 ± 1.4
Banff i score	2.4 ± 0.8
Banff t score	2.1 ± 0.8
Banff v score	0.6 ± 0.9
Banff ptc score	1.5 ± 1.3
Banff ci score	1.2 ± 0.7
Banff ct score	1.2 ± 1.0
Banff cv score	1.2 ± 1.0
Banff cg score	0.6 ± 0.9
Banff ah score	0.6 ± 0.9
C4d score	0.6 ± 1.2

Supplementary Table 2. Diagnosis at the time of biopsy from rejection patients' cohort. Data is expressed as mean ± SD. Banff score abbreviations: glomerulitis (g), interstitial inflammation (i), tubulitis (t), intimal arteritis (v) peritubular capillaritis (ptc), interstitial fibrosis (ci), tubular atrophy (ct), vascular fibrous intimal thickening (cv), glomerular basement membrane double contours (cg), arteriolar hyalinosis (ah).

Table S3

	ELISA	Biolayer interferometry	CRISPR diagnostics	qPCR
Reference	RND systems (DCX900) Hricik et al., 2013	Gandolfini et al., 2017	this paper	Altona diagnostics, RealStar Kits 021003 (CMV); 031003 (BKV)
Analyte	CXCL9 protein	CXCL9 protein	CXCL9 mRNA; BKV & CMV DNA	BKV & CMV DNA
Speed				
Assay length	4h 30min	60min	108min	85min
Hands-on time	1h 20min	10min	10min	10min
Costs				
Equipment	> $5,000 USD	> $100,000 USD (OctetRED96)	> $5,000 USD (fluorescence) $2.3 USD per test (lateral flow)	> $5,000 USD
Reagents (per test)	$5.4 USD	$1 USD	$1 USD	$20 USD
Sensitivity	11.3 pg/mL	35 pg/mL	low attomolar range	low attomolar range
POCT compatibility				
Isothermal incubation	Yes	Yes	Yes	No
Minimal equipment	No	No	Yes (lateral flow)	No
Visual output	No	No	Yes (lateral flow)	No

Supplementary Table 3. Comparison of CRISPR diagnostics with ELISA, biolayer interferometry and qPCR for the detection of CXCL9, BKV and CMV.

Table S4

Name	Sequence (5' – 3')
RPA Primer	
BKV_STA_fwd	GAAATTAATACGACTCACTATAGGCATTGCAGAGTTTC TTCAGTTAGGTCTAAGCC
BKV_STA_rev	AATTTTTAAGAAAAGAGCCCTTGGTTTGGATA
CMV_UL54_fwd	GAAATTAATACGACTCACTATAGGGCACCAGCCGAAC GTGGTGATCCGCCGATCGATGAC
CMV_UL54_rev	CTATCAGCAACTGGACCATGGCCAGAAAAATCG
CXCL9_fwd	GAAATTAATACGACTCACTATAGGTATCCACCTACAAT CCTTGAAAGACCTTAAAC
CXCL9_rev	TTAGACATGTTTGAACTCCATTCTTCAGTGTA
qPCR Primer and Probes	
CXCL9_fwd	CTTTTCCTCTTGGGCATCATCT
CXCL9_rev	AGGAACAGCGACCCTTTCTCA
CXCL9 probe	FAM-TACTGGGGTTCCTTGCACTCCAATCAGA-TAMRA
18S_fwd	GCCCGAAGCGTTTACTTTGA
18S_rev	TCCATTATTCCTAGCTGCGGTATC
18S_probe	FAM-AAAGCAGGCCCGAGCCGCC-TAMRA
Oligos for T7 synthesis of crRNAs	
T7_fwd	GAAATTAATACGACTCACTATAGG
BKV_STA_rev	CTGTGTGAAGCAGTCAATGCAGTAGCAAGTTTTAGTCC CCTTCGTTTTTGGGGTAGTCTAAATCCCTATAGTGAGT CGTATTAATTTC
CMV_UL54_rev	CGCGTCAGCGGATCCACACGGACCTCGTGTTTTAGTC CCCTTCGTTTTTGGGGTAGTCTAAATCCCTATAGTGAG TCGTATTAATTTC
CXCL9_rev	GCCCTTCCTGCGAGAAAATTGAAATCATGTTTTAGTCC CCTTCGTTTTTGGGGTAGTCTAAATCCCTATAGTGAGT CGTATTAATTTC
Synthetic targets	
CXCL9	GAAATTAATACGACTCACTATAGGATGAAGAAAAGTGG TGTTCTTTTCCTCTTGGGCATCATCTTGCTGGTTCTGAT TGGAGTGCAAGGAACCCCAGTAGTGAGAAAGGGTCG CTGTTCCTGCATCAGCACCAACCAAGGGACTATCCAC CTACAATCCTTGAAAGACCTTAAACAATTTGCCCCAAG CCCTTCCTGCGAGAAAATTGAAATCATTGCTACACTGA AGAATGGAGTTCAAACATGTCTAAACCCAGATTCAGCA GATGTGAAGGAACTGATTAAAAAGTGGGAGAAACAGG TCAGCCAAAAGAAAAAGCAAAAGAATGGGAAAAAACAT CAAAAAAAGAAAGTTCTGAAAGTTCGAAAATCTCAACG TTCTCGTCAAAAGAAGACTACATAA
Cleavage Reporter	
Lateral Flow	6FAM-mArArUrGrGrCmAmArArUrGrGrCmA-BIO
Fluorescence	RNAse ALERT V2 (Thermo)

Red indicates the T7 promoter sequence